Electronic Supporting Information

Theoretical Design of Magnetic Wires From Acene and Nanocorone Derivatives

Joan Cano[a,b]*, *Francesc Lloret*[a] *and Miguel Julve*[b]

[a]*Departament de Química Inorgància/Institut de Ciència Molecular (ICMol), Universitat de València, C/ Catedrático José Beltrán 2, 46980 Paterna, València, Spain*

[b]*Fundació General de la Universitat de València (FGUV)*

List of Contents

gions of spin density, respectively.

Figure S4. Views of calculated spin density for the BS singlet spin ground state of (a) **acene-B4** and (b) **acene-B10** models. The isodensity surfaces correspond to a cut-off value of 0.002 e bohr^{-3}. Blue and magenta isosurfaces represent positive and negative regions of spin density, respectively.

Figure S5. Spacer size dependence of the Δ_{ST} triplet-BS singlet (black) and Δ_{SQ} quintet-BS singlet (grey) energy gaps (black) and the spin contamination degree (ζ) for the triplet (blue) and BS singlet (red) wavefunctions for the diamino spacer in the **acene-A** series.

Figure S6. Spacer size dependence of the Δ_{ST} triplet-BS singlet energy gap (black) and the spin contamination degree (ζ) for the triplet (blue) and BS singlet (red) wavefunctions of the optimized models of the **acene-A** series.

Figure S7. Spacer size dependence of the Δ_{ST} triplet-BS singlet energy gap (black) and the spin contamination degree (ζ) for the triplet (blue) and BS singlet (red) wavefunctions in the **acene-C** series.

Figure S8. Spacer size dependence of the Δ_{ST} triplet-BS singlet energy gap (black) and the spin contamination degree (ζ) for the triplet (blue) and BS singlet (red) wavefunctions in the **acene-D** series.

Figure S9. Views of the calculated spin density for the BS singlet spin ground state of the (a) **acene-C1**, (b) **acene-C5** and (c) **acene-C9** models. The isodensity surfaces correspond to a cut-off value of 0.002 e bohr^{-3}. Blue and magenta isosurfaces represent the positive and negative regions of spin density, respectively.

Figure S10. Views of the calculated spin density for the BS singlet spin ground state of the (a) **acene-D1**, (b) **acene-D5** and (c) **acene-D9** models. The isodensity surfaces correspond to a cut-off value of 0.002 e bohr^{-3}. Blue and magenta isosurfaces represent the positive and negative regions of spin density, respectively.

Figure S11. Examples with N = 10 for the models from **corone-A** to **corone-C**, N being the number of fused phenyl rings in the acene group. Colour code: dark blue (copper), pale blue (nitrogen), grey (carbon) and pink (hydrogen).

Figure S12. Views of the calculated spin density for the BS singlet spin ground state of the (a) **corone-A6**, (b) **corone-A10**, (c) **corone-A20** and (d) **acene-A40** models. The isodensity surfaces correspond to a cut-off value of 0.002 e bohr^{-3}. Blue and magenta isosurfaces represent the positive and negative regions of the spin density, respectively.

Figure S13. Views of the calculated spin density for the BS singlet spin ground state of the (a) **corone-B6**, (b) **corone-B10**, (c) **corone-B20** and (d) **acene-B40** models. The isodensity surfaces correspond to a cut-off value of 0.002 e bohr^{-3}. Blue and magenta isosurfaces represent the positive and negative regions of the spin density, respectively.

Figure S14. Views of the calculated spin density for the BS singlet spin ground state of the (a) **corone-C6**, (b) **corone-C10**, (c) **corone-C20** and (d) **acene-C40** models. The isodensity surfaces correspond to a cut-off value of 0.002 e bohr^{-3}. Blue and magenta isosurfaces represent the positive and negative regions of the spin density, respectively.

Figure S15. Spacer size dependence of the Δ_{ST} triplet-BS singlet energy gap (black) and the spin contamination degree (ζ) for the triplet (blue) and BS singlet (red) wavefunctions for the **corone-A** series.

Figure S16. Spacer size dependence of the Δ_{ST} triplet-BS singlet energy gap (black) and the spin contamination degree (ζ) for the triplet (blue) and BS singlet (red) wavefunctions for the **corone-B** series.

Figure S17. Spacer size dependence of the Δ_{ST} triplet-BS singlet energy gap (black) and the spin contamination degree (ζ) for the triplet (blue) and BS singlet (red) wavefunctions for the **corone-C** series.

Figure S18. Spacer size dependence of the Δ_{ST} triplet-BS singlet energy gap (black) and the spin contamination degree (ζ) for the triplet (blue) and BS singlet (red) wavefunctions for the **acene-A** series when the calculations were done on an ideal gas, i.e., on one isolated molecule.

Table S1. Summary of more relevant structural and electronic data for the **acene-A** series.

N^a	$\Delta_{ST}{}^b$	$S^2(T)^c$	$S^2(BS)^d$	$d_{Cu...Cu}{}^e$
1	+21.3	2.0042	1.0032	8.381
2	+13.2	2.0043	1.0043	10.400
3	+12.6	2.0044	1.0065	12.559
4	+22.7	2.0048	1.0213	14.805
5	+135.6	2.1707	1.2698	17.103
6	+195.1	2.6432	1.6677	19.431
7	+201.5	2.9436	1.9525	21.788
8	+197.7	3.1605	2.1674	24.156
9	+193.6	3.3452	2.3542	26.537
10	+192.3	3.5269	2.5383	28.927

[a]Number of fused phenyl rings in the acene spacer. [b]Energy gap between the triplet and the BS singlet state (in cm^{-1}), the reference being the last one. [c]Value of the $\hat{S}^2$ operator on the triplet state. [d]Value of the $\hat{S}^2$ operator on the BS singlet state. [e]Intramolecular intermetallic distance in Å.

Table S2. Summary of more relevant structural and electronic data for the **acene-B** series.

N[a]	Δ_{ST}[b]	$S^2(T)$[c]	$S^2(BS)$[d]	$d_{Cu...Cu}$[e]
1	–6.5	2.0046	1.0042	7.490
2	–5.7	2.0050	1.0043	9.698
3	–8.4	2.0068	1.0045	11.987
4	–20.2	2.0214	1.0048	14.318
5	–133.6	2.2679	1.1695	16.684
6	–194.4	2.6670	1.6421	19.066
7	–201.0	2.9525	1.9434	21.461
8	–197.1	3.1676	2.1606	23.861
9	–193.4	3.3541	2.3451	26.268
10	–191.7	3.5383	2.5268	28.681

[a]Number of fused phenyl rings in the acene spacer. [b]Energy gap between the triplet and the BS singlet state (in cm^{-1}), the reference being the last one. [c]Value of the $\hat{S}^2$ operator on the triplet state. [d]Value of the $\hat{S}^2$ operator on the BS singlet state. [e]Intramolecular intermetallic distance in Å.

Table S3. Summary of more relevant structural and electronic data for the **acene-C** series.

N^a	$\Delta_{ST}{}^b$	$S^2(T)^c$	$S^2(BS)^d$	$d_{Cu...Cu}{}^e$
1	+21.4	2.0042	1.0033	8.406
3	+50.3	2.0044	1.0078	8.406
5	+350.7	2.1752	1.3005	8.406
7	+536.0	2.9038	1.8602	8.406
9	+530.4	3.2874	2.2226	8.406

[a]Number of fused phenyl rings in the acene spacer. [b]Energy gap between the triplet and the BS singlet state (in cm^{-1}), the reference being the last one. [c]Value of the $\hat{S}^2$ operator on the triplet state. [d]Value of the $\hat{S}^2$ operator on the BS singlet state. [e]Intramolecular intermetallic distance in Å.

Table S4. Summary of more relevant structural and electronic data for the **acene-D** series.

N^a	$\Delta_{ST}{}^b$	$S^2(T)^c$	$S^2(BS)^d$	$d_{Cu...Cu}{}^e$
1	+21.4	2.0042	1.0033	8.406
3	+35.7	2.0043	1.0052	8.406
5	+134.6	2.1812	1.2559	8.406
7	+173.1	2.9587	1.9656	8.406
9	+175.3	3.3433	2.3514	8.406

[a]Number of fused phenyl rings in the acene spacer. [b]Energy gap between the triplet and the BS singlet state (in cm^{-1}), the reference being the last one. [c]Value of the $\hat{S}^2$ operator on the triplet state. [d]Value of the $\hat{S}^2$ operator on the BS singlet state. [e]Intramolecular intermetallic distance in Å.

Table S5. Summary of more relevant structural and electronic data for the **corone-A** series.

N^a	$\Delta_{ST}{}^b$	$S^2(T)^c$	$S^2(BS)^d$	$d_{Cu...Cu}{}^e$
6	+219.1	3.1305	2.1185	11.168
8	+233.8	3.3126	2.3026	12.353
10	+260.9	3.7013	2.6933	13.619
12	+291.8	4.2393	3.2276	14.944
14	+314.5	4.7851	3.7664	16.314
16	+328.9	5.2626	4.2384	17.716
18	+338.5	5.6783	4.6510	19.143
20	+344.7	6.0645	5.0362	20.589
30	+357.5	8.0412	7.0128	27.871
40	+370.4	10.0671	9.0373	34.458

[a]Number of fused phenyl rings in the acene spacer. [b]Energy gap between the triplet and the BS singlet state (in cm^{-1}), the reference being the last one. [c]Value of the $\hat{S}^2$ operator on the triplet state. [d]Value of the $\hat{S}^2$ operator on the BS singlet state. [e]Intramolecular intermetallic distance in Å.

Table S6. Summary of more relevant structural and electronic data for the **corone-B** series.

N^a	$\Delta_{ST}{}^b$	$S^2(T)^c$	$S^2(BS)^d$	$d_{Cu...Cu}{}^e$
6	–208.4	3.0855	2.0904	8.546
8	–226.9	3.2822	2.2867	9.992
10	–260.0	3.6781	2.6837	11.512
12	–291.4	4.2125	3.2234	13.055
14	–313.7	4.7538	3.7720	14.607
16	–328.7	5.2308	4.2545	16.163
18	–337.5	5.6481	4.6749	17.719
20	–344.4	6.0359	5.0639	19.276
30	–364.4	8.0107	7.0396	27.051
40	-375.4	10.0359	9.0661	34.818

[a]Number of fused phenyl rings in the acene spacer. [b]Energy gap between the triplet and the BS singlet state (in cm^{-1}), the reference being the last one. [c]Value of the $\hat{S}^2$ operator on the triplet state. [d]Value of the $\hat{S}^2$ operator on the BS singlet state. [e]Intramolecular intermetallic distance in Å.

Table S7. Summary of more relevant structural and electronic data for the **corone-C** series.

N^a	$\Delta_{ST}{}^b$	$S^2(T)^c$	$S^2(BS)^d$	$d_{Cu...Cu}{}^e$
6	+221.4	3.0905	2.0806	7.190
8	+233.4	3.2483	2.2409	7.263
10	+259.2	3.6189	2.6130	7.277
12	+287.6	4.1628	3.1526	7.273
14	+300.1	4.7309	3.7137	7.260
16	+322.9	5.2248	4.2006	7.255
18	+330.7	5.6492	4.6219	7.245
20	+335.6	6.0379	5.0098	7.236
30	+352.4	8.0124	6.9848	7.205
40	+358.2	10.0377	9.0101	7.186

[a]Number of fused phenyl rings in the acene spacer. [b]Energy gap between the triplet and the BS singlet state (in cm^{-1}), the reference being the last one. [c]Value of the $\hat{S}^2$ operator on the triplet state. [d]Value of the $\hat{S}^2$ operator on the BS singlet state. [e]Intramolecular intermetallic distance in Å.

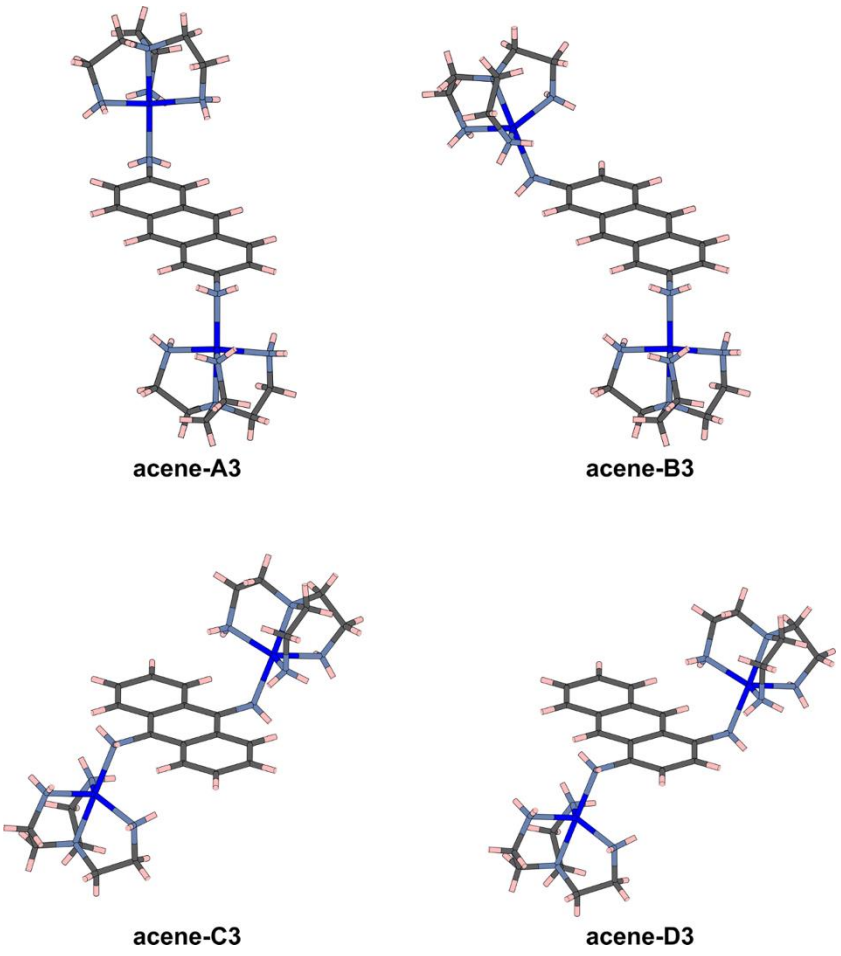

Figure S1. Examples with *N* = 3 for models from **acene-A** to **acene-D**, *N* being the number of fused phenyl rings in the acene group. Colour code: dark blue (copper), pale blue (nitrogen), grey (carbon) and pink (hydrogen).

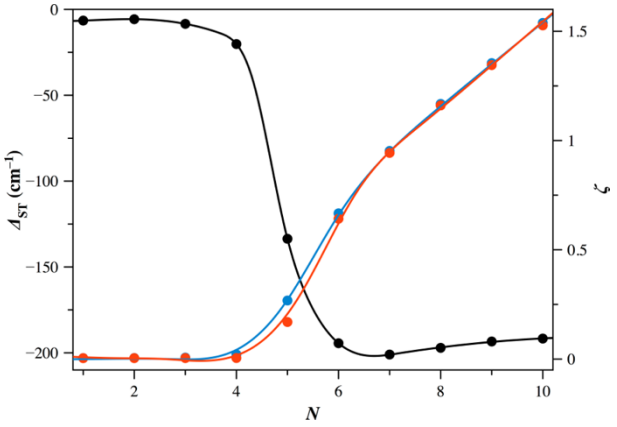

Figure S2. Spacer size dependence of the Δ_{ST} triplet-BS singlet energy gap (black) and the spin contamination degree (ζ) for the triplet (blue) and BS singlet (red) wavefunctions for the **acene-B** series.

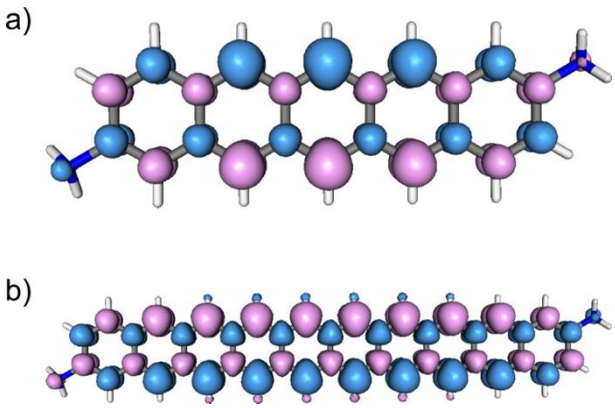

Figure S3. Views of the calculated spin density for the BS singlet spin ground state of diamine spacer of the (a) **acene-A5** and (b) **acene-A10** models. The isodensity surfaces correspond to a cut-off value of 0.002 e bohr^{-3}. Blue and magenta isosurfaces represent positive and negative regions of the spin density, respectively.

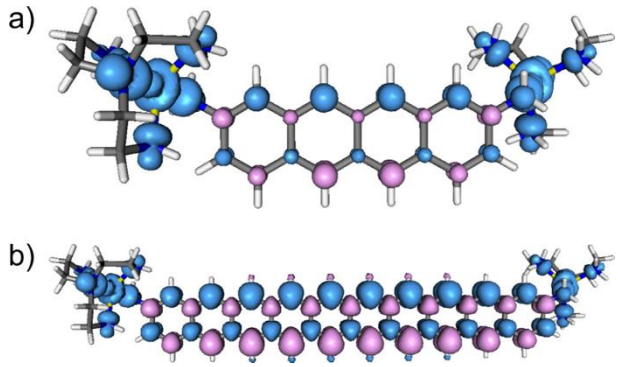

Figure S4. Views of the calculated spin density for the BS singlet spin ground state of the diamine spacers in the (a) **acene-B4** and (b) **acene-B10** models. The isodensity surfaces correspond to a cut-off value of 0.002 e bohr^{-3}. Blue and magenta isosurfaces represent the positive and negative regions of the spin density, respectively.

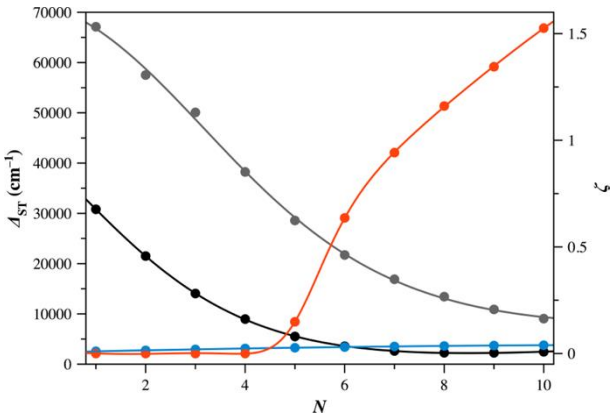

Figure S5. Spacer size dependence of the Δ_{ST} triplet-BS singlet (black) and Δ_{SQ} quintet-BS singlet (grey) energy gaps (black) and the spin contamination degree (ζ) for the triplet (blue) and BS singlet (red) wavefunctions for the diamino spacer in the **acene-A** series.

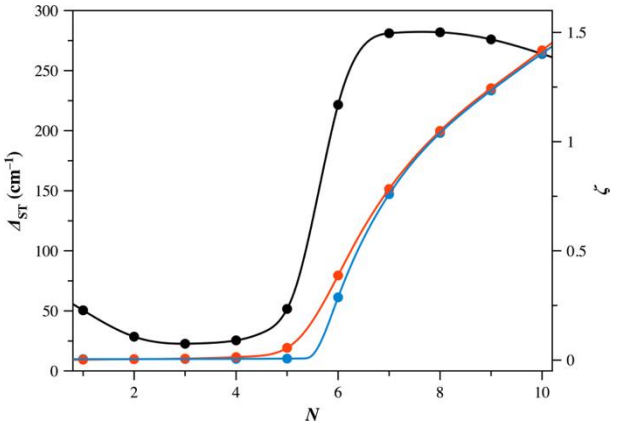

Figure S6. Spacer size dependence of the Δ_{ST} triplet-BS singlet energy gap (black) and the spin contamination degree (ζ) for the triplet (blue) and BS singlet (red) wavefunctions of the optimized models of the **acene-A** series.

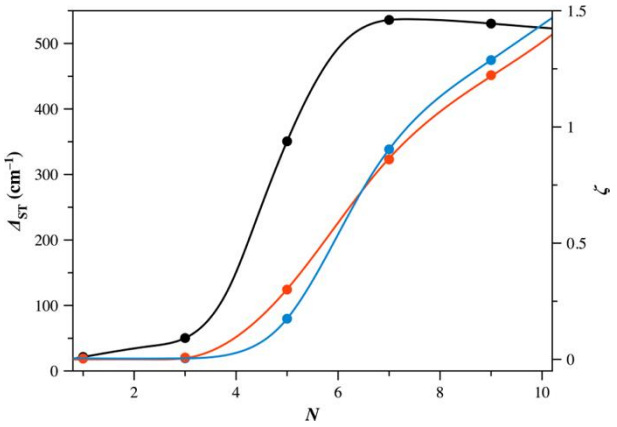

Figure S7. Spacer size dependence of the Δ_{ST} triplet-BS singlet energy gap (black) and the spin contamination degree (ζ) for the triplet (blue) and BS singlet (red) wavefunctions in the **acene-C** series.

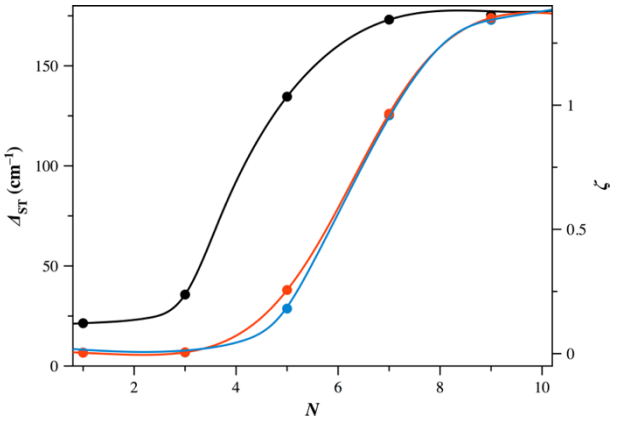

Figure S8. Spacer size dependence of the Δ_{ST} triplet-BS singlet energy gap (black) and the spin contamination degree (ζ) for the triplet (blue) and BS singlet (red) wavefunctions in the **acene-D** series.

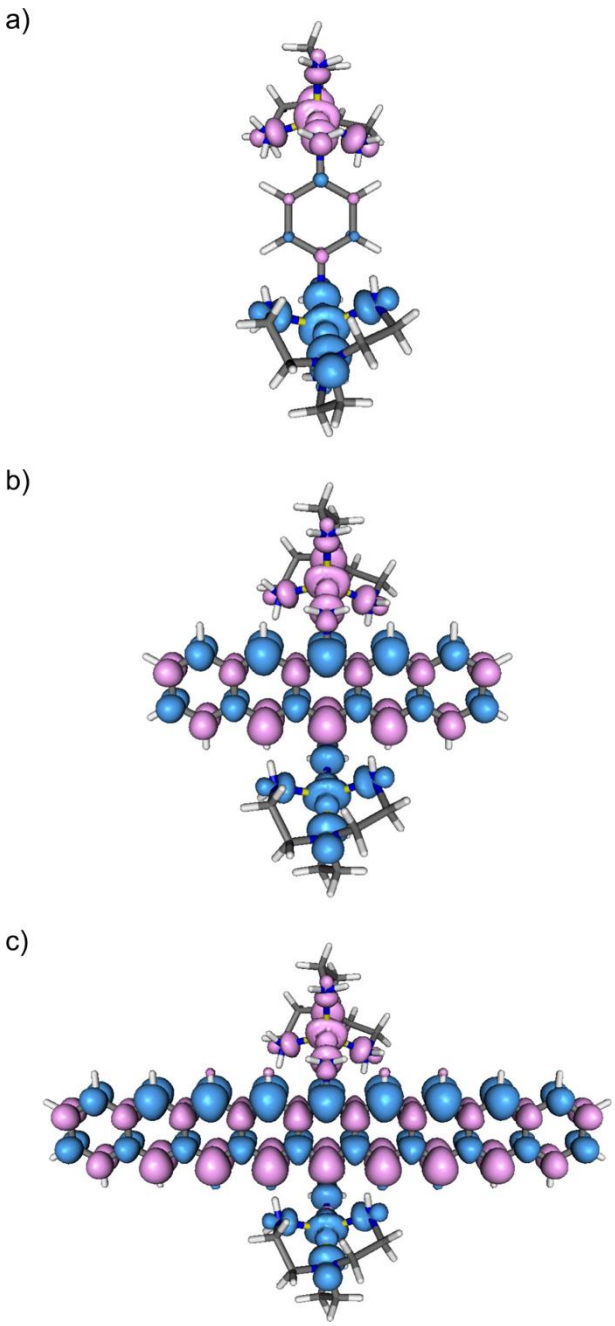

Figure S9. Views of the calculated spin density for the BS singlet spin ground state of the (a) **acene-C1**, (b) **acene-C5** and (c) **acene-C9** models. The isodensity surfaces correspond to a cut-off value of 0.002 e bohr^{-3}. Blue and magenta isosurfaces represent the positive and negative regions of the spin density, respectively.

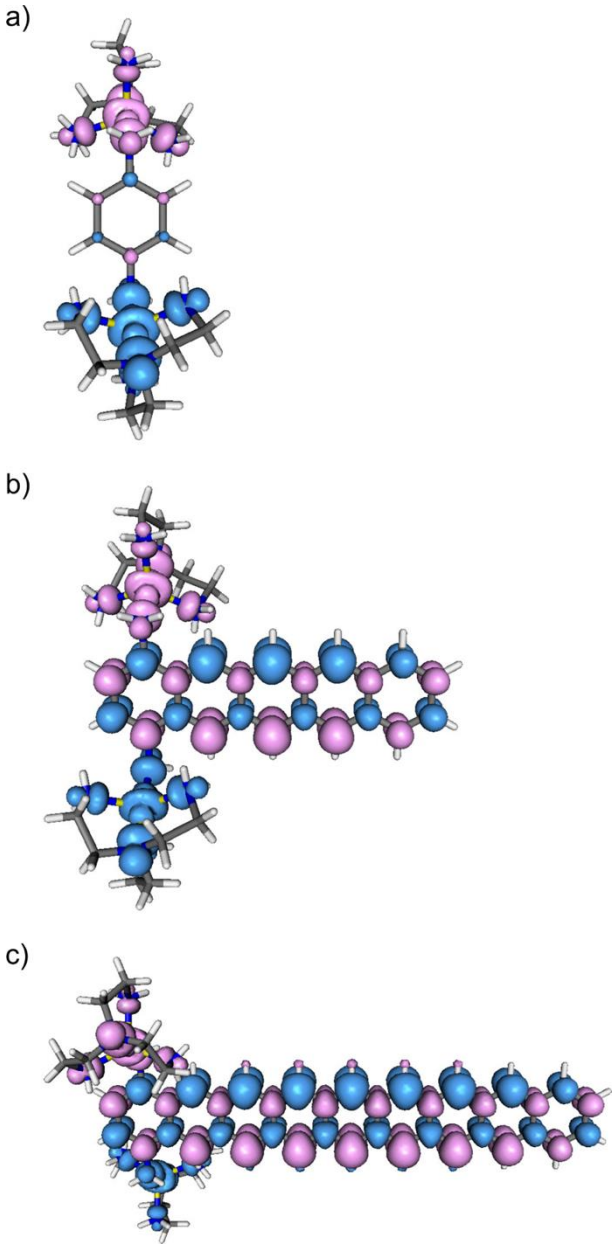

Figure S10. Views of the calculated spin density for the BS singlet spin ground state of the (a) **acene-D1**, (b) **acene-D5** and (c) **acene-D9** models. The isodensity surfaces correspond to a cut-off value of 0.002 e bohr^{-3}. Blue and magenta isosurfaces represent the positive and negative regions of the spin density, respectively.

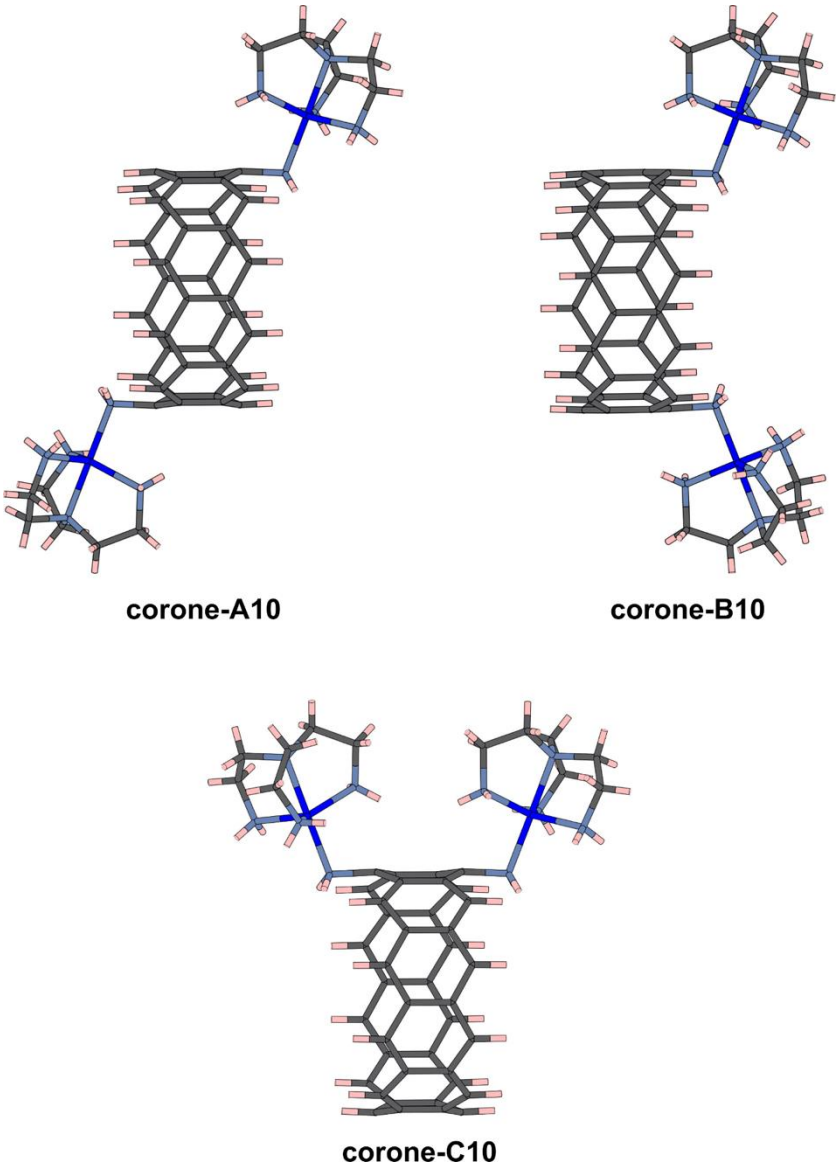

Figure S11. Examples with *N* = 10 for models from **corone-A** to **corone-C**, *N* being the number of fused phenyl rings in the acene group. Colour code: dark blue (copper), pale blue (nitrogen), grey (carbon) and pink (hydrogen).

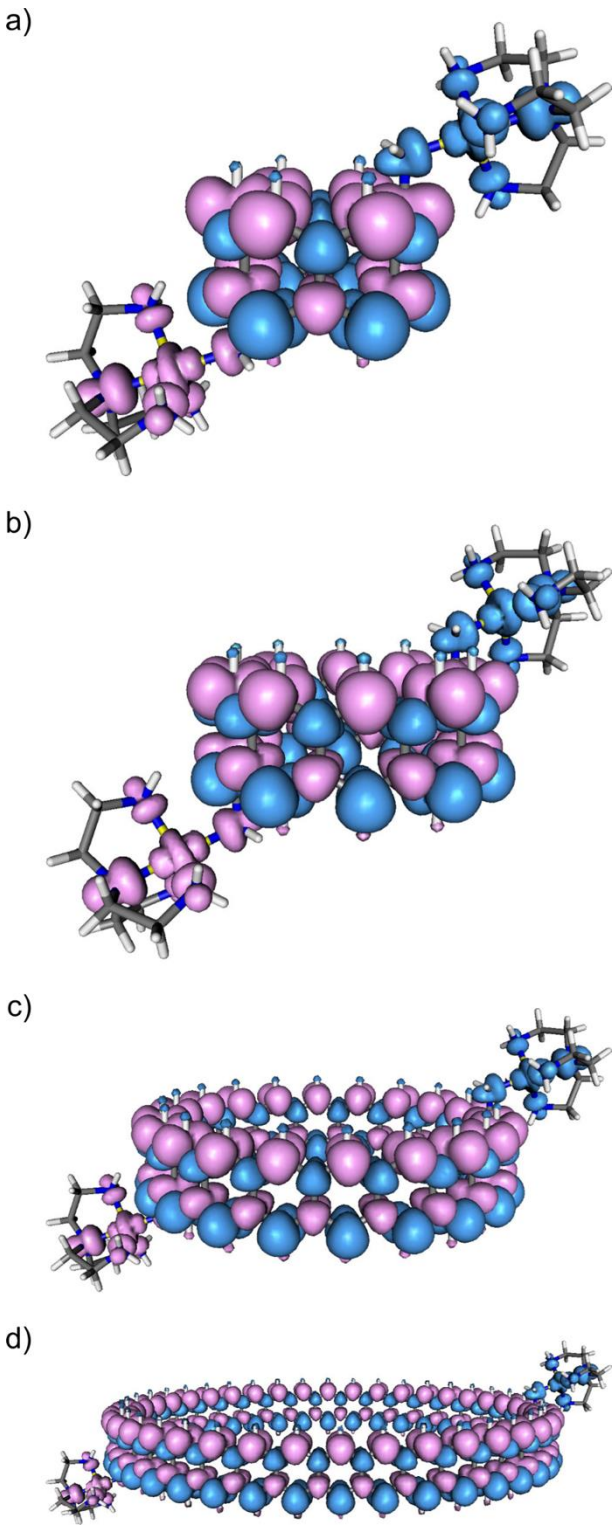

Figure S12. Views of the calculated spin density for the BS singlet spin ground state of the (a) **corone-A6**, (b) **corone-A10**, (c) **corone-A20** and (d) **acene-A40** models. The isodensity surfaces correspond to a cut-off value of 0.002 e bohr^{-3}. Blue and magenta isosurfaces represent the positive and negative regions of the spin density, respectively.

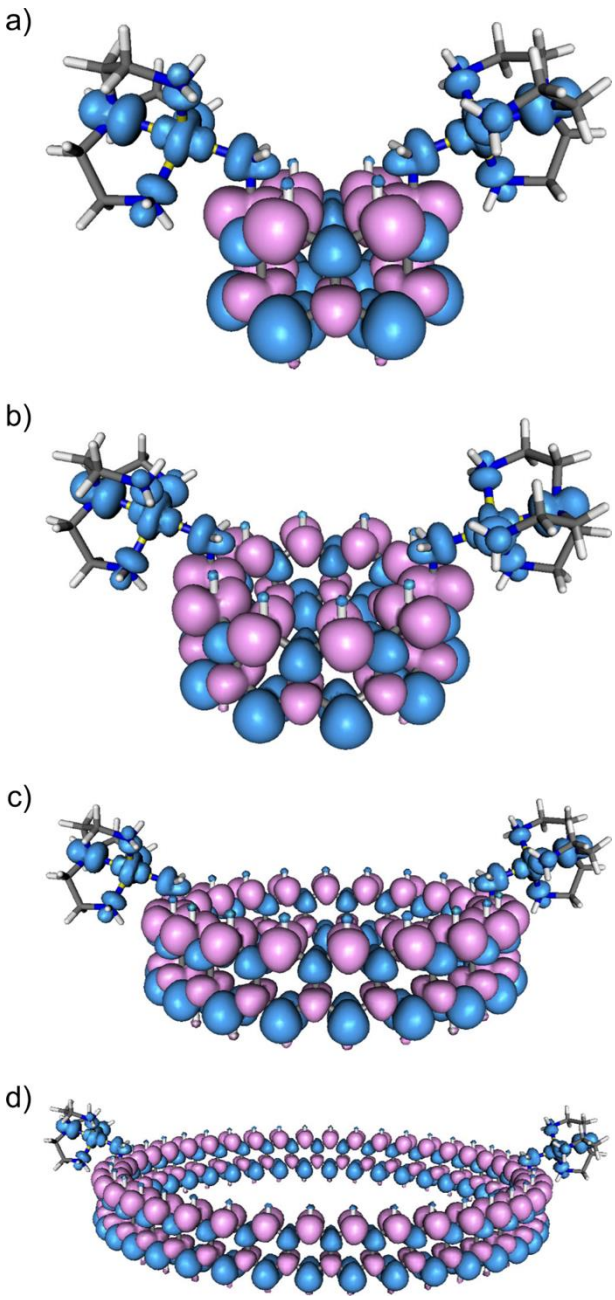

Figure S13. Views of calculated the spin density for the BS singlet spin ground state of the (a) **corone-B6**, (b) **corone-B10**, (c) **corone-B20** and (d) **acene-B40** models. The isodensity surfaces correspond to a cut-off value of 0.002 e bohr^{-3}. Blue and magenta isosurfaces represent the positive and negative regions of the spin density, respectively.

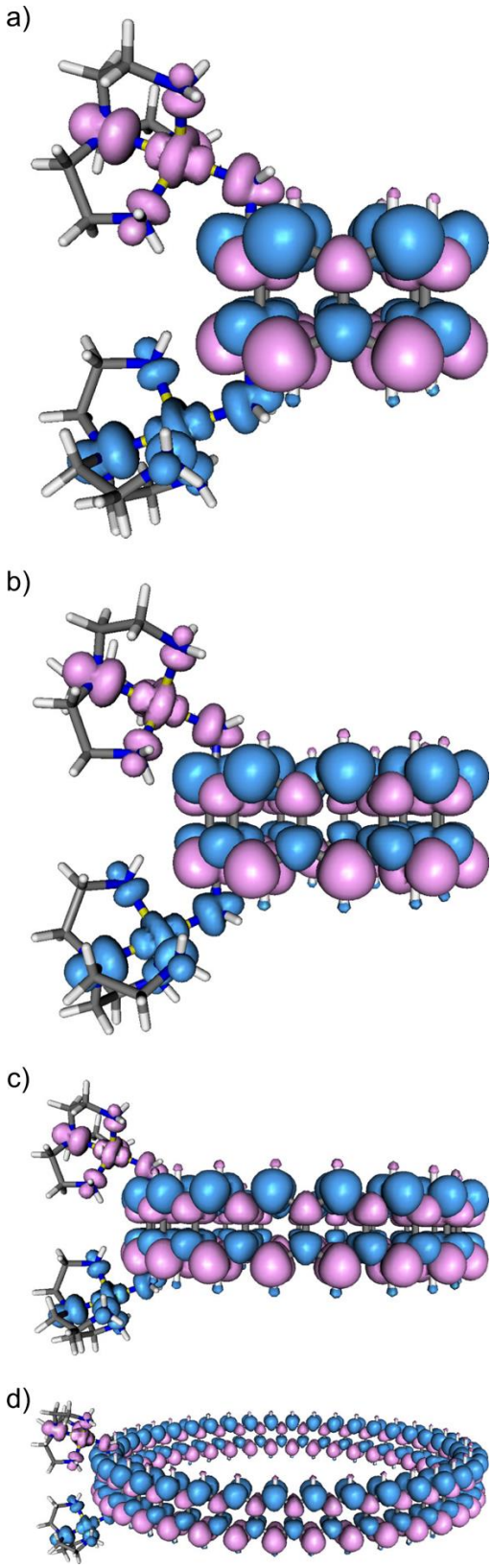

Figure S14. Views of calculated the spin density for the BS singlet spin ground state of the (a) **corone-C6**, (b) **corone-C10**, (c) **corone-C20** and (d) **acene-C40** models. The isodensity surfaces correspond to a cut-off value of 0.002 e bohr^{-3}. Blue and magenta isosurfaces represent the positive and negative regions of the spin density, respectively.

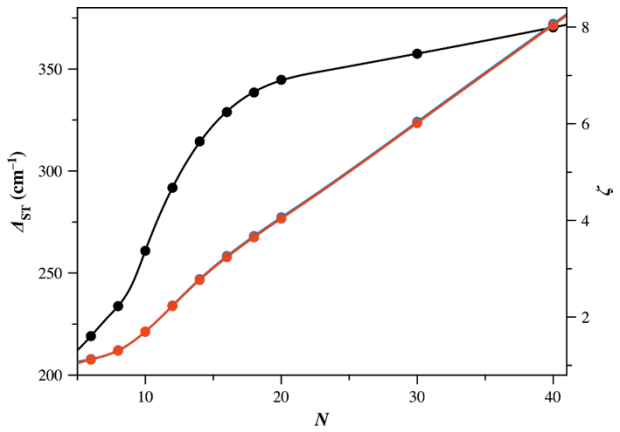

Figure S15. Spacer size dependence of the Δ_{ST} triplet-BS singlet energy gap (black) and the spin contamination degree (ζ) for the triplet (blue) and BS singlet (red) wavefunctions for the **corone-A** series.

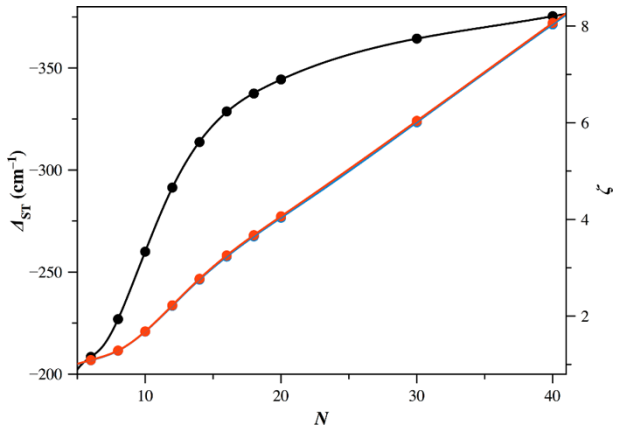

Figure S16. Spacer size dependence of the Δ_{ST} triplet-BS singlet energy gap (black) and the spin contamination degree (ζ) for the triplet (blue) and BS singlet (red) wavefunctions for the **corone-B** series.

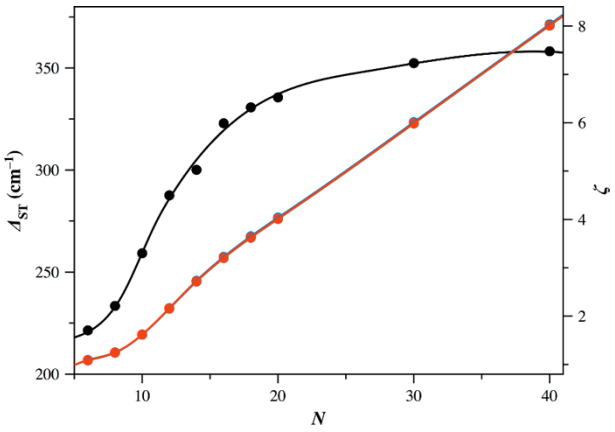

Figure S17. Spacer size dependence of the Δ_{ST} triplet-BS singlet energy gap (black) and the spin contamination degree (ζ) for the triplet (blue) and BS singlet (red) wavefunctions for the **corone-C** series.

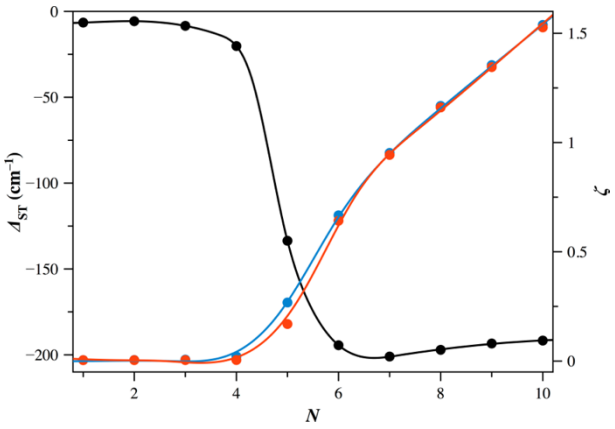

Figure S18. Spacer size dependence of the Δ_{ST} triplet-BS singlet energy gap (black) and the spin contamination degree (ζ) for the triplet (blue) and BS singlet (red) wavefunctions for the **acene-A** series when the calculations were done on an ideal gas, i.e., on one isolated molecule.